

# Mathematical Modeling of Two-Dimensional Diffraction Analysis in Anisotropic Media

## 비등방성 매질에서의 2차원적 회절현상의 수학적 모델링

Yeong Jee Chung\*, Kyo Young Jin\*

정 영 지, 진 교 영

### ABSTRACT

Mathematical model for two-dimensional diffraction for anisotropic media is derived. Here, the velocity surface is assumed to be a parabola so that the parabolic anisotropies and Fresnel approximations method can be applied.

The computer simulation of diffraction response of the SAW IF bandpass filter for  $128^\circ$  rotated  $\text{LiNbO}_3$  using the above-mentioned method is done on VAX 8550 in FORTRAN.

The result is compared with "no diffraction" case and the effect of diffraction is clearly demonstrated. Furthermore, it is demonstrated that the actual response of the SAW IF band pass filter for  $128^\circ$   $\text{LiNbO}_3$  agrees reasonably well with the simulation result.

### 요 약

본 논문에서는 비등방성 매질에서의 2차원적 회절현상을 수학적으로 모델링하였다. 비등방성 매질의 2차 포물선 근사법과 프레즈넬 근사법을 적용하기 위하여 전파방향에 따른 표면파 속도의 역수를 포물선으로 가정하였다.

$128^\circ$  Rotated  $\text{LiNbO}_3$  기판을 사용한 SAW IF Bandpass Filter에서의 회절현상을 모의 실험하여 그 결과를 회절현상이 없는 이상적인 경우와 비교하였다. 또한 전산화 모의 실험 결과와 실제로 제작된 SAW Filter 측정결과를 비교하여  $\text{LiNbO}_3$  기판을 사용한 SAW Filter에서도 프레즈넬 근사법이 대체적으로 일치하는 것을 알 수 있었다.

## I. INTRODUCTION

Ideally, Acoustic Surface Wave band pass

filters can be designed by applying straight forward Fourier Transform pair and digital filter procedures since an interdigital transducer can be made to be an excellent representation of a transversal filter.

Unfortunately the phenomenon of diffraction or beam spreading severely affect the filter

\* Samsung Advanced Institute of Technology, Materials Devices Research Center

P. O. Box 111 Suwon Kyeongkido

삼성종합기술원 소재부서 연구실

response characteristics. The effect of diffraction on Surface Acoustic Wave band pass filter performance is to degrade the filter shape factor and stop band rejection. Finger overlap apodization results in diffraction variation which destroy the ideal Fourier-Transform relationship. Regions where the finger overlap is small yield significantly more diffraction loss than that for the longer overlap. This results in the necessity for compensation in order to get the desired response.

The two most important methods employed to calculate the effects of anisotropic surface acoustic wave diffraction are the techniques using the Parabolic-Anisotropy and Fresnel approximation and the Angular Spectrum of Waves technique.

The parabolic anisotropy method has been shown to be useful for SAW velocity characteristics that can be well approximated by a parabola and for propagation regions far enough from a transducer such that the Fresnel condition can be satisfied.

The angular spectrum of waves technique has been demonstrated to be an accurate method for nonparabolic cases and is limited primarily by its dependence on detailed velocity versus angle information.

It is important to note that diffraction of Surface Acoustic Wave is a physical consequence of their propagation and can vary greatly depending upon which anisotropic substrate is chosen for a given application. The fact that diffraction effects are unique to the particular anisotropic substrate can be seen from the slowness curve which is the plot for the reciprocal of phase velocity as a function of angle of propagation direction.

The form of the slowness curve will depend on the substrate material and the orientation of the surface normal.

The slowness curve for the particular substrate material is important since diffraction considerations and permissible misalignment tolerances require knowledge of propagation

conditions for wave vectors oriented at an angle to the design pure-mode direction. The Quartz whose slowness surface can well be approximated by a parabola is a good example to which the parabolic anisotropy and Fresnel approximation can be applied. For other materials, it is generally believed that this approximation cannot be used. Therefore, other methods such as angular spectrum of waves technique by Kharusi and Farnell [4], geometrical theory of diffraction by Rada-sky and Matthaehi [7], and asymptotic technique as developed by Tan and Flory [6] are employed for diffraction analyses. It is worth noting that the technique developed by Tan and Flory reduces the computation time considerably but it does not by any means give a satisfactory results as far as the frequency response is concerned.

In this paper, the parabolic anisotropy and Fresnel approximation method under the assumption that the velocity surface can be well approximated by a parabola, is used to calculate the frequency response of the band pass filter. The mathematical model for two-dimensional diffraction in anisotropic media, is derived and by using this model, the frequency response of SAW IF bandpass filter with diffraction is obtained through computer simulation done on VAX8550 in FORTRAN programming language. The result is plotted and compared with that of "no-diffraction" case. Furthermore, the simulation result is compared with the response of the actual device fabricated on  $128^\circ$  Rotated  $\text{LiNbO}_3$  to examine whether the parabolic anisotropy and the Fresnel approximation method is applicable for the diffraction analysis of the SAW IF bandpass filter for  $128^\circ$  Rotated  $\text{LiNbO}_3$  and to what extent.

## II. DIFFRACTION THEORY

### i. Isotropic case

In an isotropic diffraction case [1], the direction of propagation coincides with the direction of the phase and group velocity vectors as shown in Fig.1.(a).

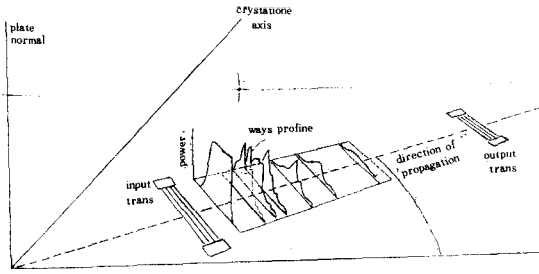


Fig. 1.(a) - an isotropic diffraction case

Assuming that the transducers can be represented by line sources having a constant amplitude over their length and all the acoustic energy is confined to the surface, then the propagation of acoustic surface wave on an isotropic substrate is similar to the classical optical case of light illuminating an infinitesimally narrow slit of length  $L$ . If a coordinate system is chosen so that the transducer is centered at the origin along  $X$  axis,  $Z$  is the perpendicular distance from the transducer to an observation point, and  $\lambda$  the appropriate wavelength, then we can define parameters  $N_{\pm}$  such that,

$$N_{+} = \frac{X - L/2}{\sqrt{\lambda z/2}}, \quad N_{-} = \frac{X + L/2}{\sqrt{\lambda z/2}}$$

For field points near the  $Z$  axis and not very close to the  $X$  axis, i.e.,  $L/Z < 1$ , the kirchhoff integral may be approximated by the well-known Fresnel integral,

$$A(X, Z) = 1/\sqrt{2} \int_{N_{-}}^{N_{+}} \exp(-j\pi v^2/2) dv \quad (1)$$

where  $A(X, Z)$  is the strain amplitude at an observation point  $(X, Z)$ .

Let  $\hat{L} = L/\lambda$ ,  $\hat{Z} = Z/\lambda$ ,  $\hat{X} = X/\lambda$ , so that

$$N_{+} = \frac{\hat{X} - \hat{L}/2}{\sqrt{\hat{z}/2}}, \quad N_{-} = \frac{\hat{X} + \hat{L}/2}{\sqrt{\hat{z}/2}}$$

The beam profiles of Fig.1.(a) show the sequence of patterns typical of isotropic diffraction.

First, very close to the surface, the appearance of small ripples. Second, one or more pronounced cleavages. Third, the emergence of the final peak. Fourth, a tall, distinct final peak. Fifth, the far-field pattern. A distinction between the near field or Fresnel region and the far-field or Fraunhofer region can be made. A convenient figure for approximately defining the demarcation between these two regions is the "far-field length",  $\hat{Z}_f = \hat{L}^2$  which is the distance  $Z$  at which the final peak has begun to descend monotonically

### 2. Anisotropic case

Unlike the isotropic case, the direction of the phase and group velocity vectors coincide only for specific values of  $\Theta$  defined as pure-mode axis. Thus the acoustic beam is shown propagating off at an angle  $\phi$ , the power flow angle, with respect to the center line between the two transducers.(Fig.1.(b))

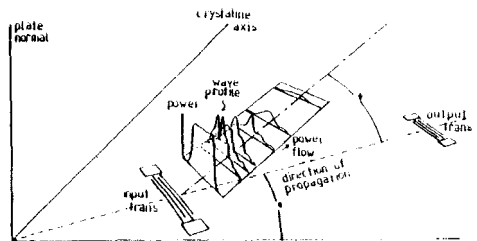


Fig. 1.(b) - an anisotropic diffraction case

A direct measure of the seriousness of this effect is  $d\phi/d\Theta$ , the slope of the power flow angle. Anisotropy introduces other interrelated complications: not only is the severity of beam steering peculiar to both the orientation direction and the material chosen, but the diffraction patterns are also unique to the particular anisotropy and do not occur in the normal isotropic manner.

#### 2.1. Parabolic anisotropic case

The power flow angle wave is related to the derivative of the velocity by:

$$\tan \phi = 1/v_0 \cdot dv/d\theta \tag{12}$$

For small deviations near a pure mode axis, the small angle approximation for the tangent implies

$$\phi = 1/v_0 \cdot dv/d\theta \tag{13}$$

where  $v_0$  is the pure mode velocity.

A theory developed by Cohen [2] is useful for calculating diffraction fields when the velocity anisotropy on or near pure mode axis can be approximated by a parabola. By using a small angle approximation, Cohen showed that for certain cases, the higher orders of the expression for the velocity could be neglected past the second order. That is,

$$\frac{v(\theta)}{v_0} \approx 1 + \gamma/2 \cdot (\theta - \theta_0)^2 \tag{14}$$

where  $\gamma$  is an anisotropy parameter and  $\theta_0$  is the angular orientation of the pure mode axis. Furthermore, for these conditions the acoustic power flow vector deviates from the pure mode axis by the angle

$$\phi = \gamma(\theta - \theta_0) \equiv \gamma\theta' \tag{15}$$

, which is in complete agreement with (3). By comparing these approximations to an exact solution for electromagnetic diffraction in uniaxially anisotropic media, he showed that the diffraction integral reduces to Fresnel's integral with the following change

$$\hat{z}' = \hat{z} \sqrt{1 + \gamma}$$

Here, the absolute sign indicates that diffraction is either accelerated or retarded depending on the value and sign of  $\gamma$ . Therefore, by substituting  $z'$  for the actual distance  $Z$ , the new limits for Fresnel integral which was previously defined, become

$$N^{(+) = \frac{\hat{X} + \hat{L}/2}{\sqrt{\hat{z} \sqrt{1 + \gamma}/2}}, \quad N^{(-) = \frac{\hat{X} - \hat{L}/2}{\sqrt{\hat{z} \sqrt{1 + \gamma}/2}}$$

where the parameters are scaled to  $\lambda$ , the wavelength along the pure mode axis. The far-field distribution is [3]

$$E(X, Z) = (A(X, Z))^{1/2} \frac{\hat{L}^2}{\hat{z} \sqrt{1 + \gamma}} \frac{\sin^2 \pi\beta}{(\pi\beta)^2} \tag{16}$$

where

$$\beta = \frac{\hat{X} \hat{L}}{\hat{z} \sqrt{1 + \gamma}}$$

It is to note that an excellent agreement is to be expected between the parabolic theory and experimental results only if velocity anisotropy can be approximated by a parabola. Otherwise, different techniques must be employed.

### 2.2. Angular Spectrum of Waves Anisotropic case

An angular spectrum of waves technique was originally developed for the diffraction of light or acoustic bulk waves at plane apertures in homogeneous but highly anisotropic crystals. This technique was then applied to surface wave diffraction by Kharusi and Farnell.[4] Their theory is valid for both the near and far fields, and for any direction including off-axis orientations. Its only limitation is the requirement of accurate knowledge of velocity value for the surface of interest.

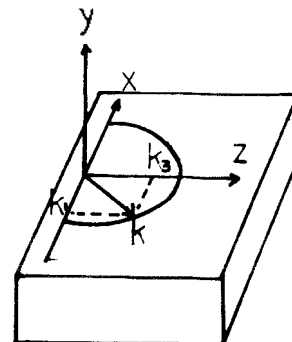


Fig. 2. A coordinate System on an anisotropic substrate.

Referring to Fig.2,  $A(X,Z)$  at a field point  $(X,Z)$ ,  $Z > 0$ , with interdigital transducer aperture of length  $L$  lying along the  $X$  axis and extending from  $-L/2$  to  $+L/2$ , can be represented by

$$A(X, Z) = \int_{-\infty}^{\infty} a(k_1) \exp[j(k_1 X + k_3 Z)] dk_1 \quad (7)$$

given that

$$k(k) = 2\pi\nu/v(k)$$

where

$$[k_3(k_1)]^2 = [k(k)]^2 - k_1^2$$

$\nu$  is the frequency,  $v(\hat{k})$  is the phase velocity in the wave vector direction  $\hat{k}$  and  $k$  is the magnitude of  $k$ . It is apparent that,

$$A(X, 0) = \int_{-\infty}^{\infty} a(k_1) \exp(jk_1 X) dk_1 \quad (8)$$

and that through Fourier inversion,

$$A(X, Z) = 1/(2\pi) \int_{-\infty}^{\infty} \int_{-L/2}^{L/2} a(X') \exp[jk_1(X-X') + jk_3(k_1)(Z)] dk_1 dx' \quad (9)$$

where  $X'$  varies across the aperture or transducer region, since  $f(x, 0)$  is considered zero outside this aperture, the above equation can be analytically integrated over  $X'$  to give

$$A(X, Z) = 1/\pi \int_{-\infty}^{\infty} 1/k_1 \cdot \sin(k_1 L/2) \exp[jk_1 X + jk_3(k_1)(Z)] dk_1 \quad (10)$$

The above integral is computed numerically for each field point. The angular spectrum of waves technique can be used to predict even the fine structure of a diffraction pattern on a highly nonparabolic velocity surface, including profile asymmetry due to beam steering. Unfortunately however, limitations in the accurate knowledge of velocity surface prevents such

excellent agreement for a certain restricted class of materials.

### III. MATHEMATICAL MODELING OF TWO-DIMENSIONAL DIFFRACTION IN ANISOTROPIC MEDIA

In three-dimensional diffraction case (Fig.3), the derivation starts with the angular spectrum of waves approach, using an ellipsoidal slowness surface, as present in uniaxial optic materials, to represent the anisotropy.

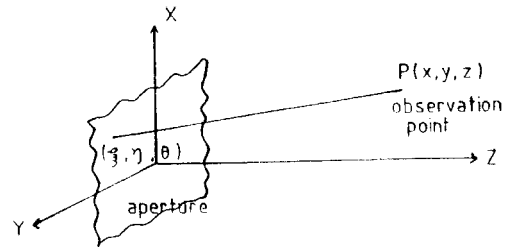


Fig. 3 a coordinate system for three-dimensional diffraction analysis

By a transformation the problem becomes isotropic, and has an exact solution. By making some approximations this solution is then simplified into the Fresnel diffraction form. The result is given here without derivation. The detailed derivation can be found in [5]. The result is,

$$f(x, y, z) = \frac{j\beta \exp(j\beta z)}{2\pi z(1-\gamma)} \int_{-\infty}^{\infty} \int_{-\infty}^{\infty} f(\xi, \eta, 0) \exp\left\{j\beta \left[ \frac{x-\xi}{2z(1-\gamma)} + \frac{y-\eta}{2z(1-\gamma)} \right]^2 \right\} d\xi d\eta \quad (11)$$

The expression given above is extended to two-dimensional case by assuming one variation is constant ( $Y$  variation). The two-dimensional diffraction however, can be derived directly by the following six steps:

**1. Obtain the angular spectrum of waves equation**

Assume the field of interest is scalar.

$$f(x, z) = \int_{-\infty}^{\infty} F(k_x) \exp[-j(k_x X + k_z(k_x) Z)] dk_x \quad (1)$$

$$f(x, 0) = \int_{-\infty}^{\infty} F(k_x) \exp[-j k_x X] dk_x \quad (2)$$

where  $F(k_x)$  is the plane wave amplitude coefficient and  $k_z(k_x)$  is the propagation medium. Now take the Fourier Transform,

$$F(k_x) \approx 1/(2\pi) \int_{-\infty}^{\infty} f(\xi, 0) \exp[j k_x \xi] d\xi \quad (3)$$

So the field is given as

$$f(x, z) = 1/(2\pi) \int_{-\infty}^{\infty} f(\xi, 0) \left[ \int_{-\infty}^{\infty} \exp[-j(k_x(x-\xi) + k_z(k_x)z)] dk_x \right] d\xi \quad (4)$$

where

$$k_z(k_x) = \begin{cases} \sqrt{\beta^2 - k_x^2/\epsilon_r} & \text{for } k_x^2 \leq \epsilon_r \beta^2 \\ -j\sqrt{k_x^2/\epsilon_r - \beta^2} & \text{for } k_x^2 \geq \epsilon_r \beta^2 \end{cases}$$

$\beta, \epsilon_r$  are constants and ellipsoidal slowness surface is assumed.

**2. Convert the integral to the isotropic form**

Let  $k_x(k_x) = \sqrt{\epsilon_r} k_x$ ,  $Z = z/\sqrt{\epsilon_r}$

$$X = x/\xi, B = \sqrt{\epsilon_r} \beta$$

so that  $k_x^2 = k_x^2/B^2$  and  $x^2 = z^2/R^2$

Then

$$f(x, z) = 1/(2\pi) \int_{-\infty}^{\infty} f(\xi, 0) \left[ \int_{-\infty}^{\infty} \exp[-j(k_x X + k_z(k_x) Z)] dk_x \right] d\xi \quad (5)$$

**3. Evaluate the integral in the bracket**

$$\int_{-\infty}^{\infty} \exp[-j(k_x X + k_z(k_x) Z)] dk_x = -j\pi \frac{BZ}{R} H_1^{(2)}(BR) \quad (6)$$

where  $H_1^{(2)}(BR)$  is the Hankel function.

**4. Substitute this result into the field equation**

Assuming the velocity surface can be approximated by a parabola,

$$f(x, z) = 1/(2\pi) \int_{-\infty}^{\infty} f(\xi, 0) \exp[-j\pi] \frac{BZ}{R} H_1^{(2)}(BR) d\xi$$

or

$$f(x, z) = -j\beta/2 \int_{-\infty}^{\infty} f(\xi, 0) \frac{Z}{R} H_1^{(2)}(BR) d\xi \quad (8)$$

where,

$$R = \sqrt{(x/\xi)^2 + z^2/\epsilon_r}, B = \sqrt{\epsilon_r} \beta$$

**5. Next, assume that R is large compared to a wavelength**

$$H_1^{(2)}(x) \approx \sqrt{2/\pi x} \exp[-j(x - 3\pi/4)] - j \exp[j\pi/4] \sqrt{2/\pi x} \exp[-jx]$$

so that

$$f(x, z) = \exp[j\pi/4] \sqrt{\beta/2\pi\sqrt{\epsilon_r}} \int_{-\infty}^{\infty} f(\xi, 0) \frac{Z}{R} \exp[-jBR] d\xi \quad (9)$$

**6. Utilize the Fresnel approximation**

For small angles,

so,

$$f(x, z) \sim \exp(j\pi/4) \sqrt{\frac{\beta \epsilon_r}{2\pi^2}} \exp(-j\beta z) \int_{-\infty}^{\infty} f(\xi, 0) \exp\{-j\beta(x-\xi)^2 \epsilon_r / 2z\} d\xi \quad (20)$$

with  $\epsilon_r = \frac{1}{|1+\gamma|}$

$$f(x, z) \sim \exp(j\pi/4) \sqrt{\frac{\beta}{2\pi z |1+\gamma|}} \exp(-j\beta z) \int_{-\infty}^{\infty} f(\xi, 0) \exp\left\{-j\frac{\beta(x-\xi)^2 \epsilon_r}{2z |1+\gamma|}\right\} d\xi \quad (21)$$

The radiated field can be considered the superposition of a two-dimensional point-source field pattern radiated by each point in the aperture. This result can now be used for the case of a uniform aperture.

Let

$$x - \xi = \frac{\sqrt{\pi z |1+\gamma|}}{\beta} v$$

then

$$f(x, y) = \frac{\exp(j\pi/4) \exp(-j\beta z)}{\sqrt{2}} \int_{-\infty}^{\infty} f\left(\frac{\sqrt{\pi z |1+\gamma|}}{\beta} v, 0\right) \exp(-j\pi/2 \cdot v^2) dv \quad (22)$$

when

$$f(\xi, 0) = \begin{cases} 1 & -A/2 < \xi < A/2 \\ 0 & \text{otherwise} \end{cases}$$

and

$$f(x, z) = \frac{\exp(j\pi/4) \exp(-j\beta z)}{\sqrt{2}} \int_{-v}^{v} \exp(-j\pi/2 \cdot v^2) dv \quad (23)$$

where

$$v \pm = \sqrt{\frac{\beta}{\pi z |1+\gamma|}} (x \pm A/2)$$

Now define the Fresnel integral functions as

$$E^*(x) = Ci(x) - j Si(x) = \frac{1}{\sqrt{2\pi}} \int_0^x \frac{\exp(-jt)}{\sqrt{t}} dt = \int_0^{\sqrt{x/\pi}} \exp(-j\pi/2 \cdot v^2) dv \quad (24)$$

so

$$f(x, z) = \frac{\exp(j\pi/4) \exp(-j\beta z)}{\sqrt{2}} \left\{ E^* \left[ \frac{(x+A/2)\sqrt{\pi}}{z/\pi |1+\gamma|} \right] - E^* \left[ \frac{(x-A/2)\sqrt{\pi}}{z/\pi |1+\gamma|} \right] \right\} \quad (25)$$

where  $\lambda = \frac{2\pi}{\beta}$  is the wavelength.

$$f(x, z) = \frac{\exp(j\pi/4) \exp(-j\beta z)}{\sqrt{2}} \left\{ E^*(T+) - E^*(T-) \right\} \quad (26)$$

$$T \pm = \frac{\pi F (x \pm A/2)^2}{z |1+\gamma|} \quad f/f_0$$

F: Normalized frequency,  $f/f_0$ . The equation (26) gives the value of the radiated field at each point on the line receiver. This is then integrated by the line receiver to give the response.(Fig.4)

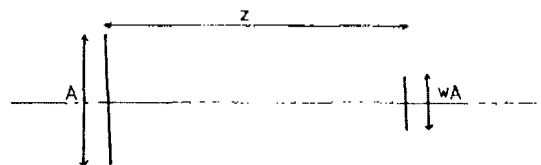


Fig. 4 single transmitter-receiver pair, with symmetrical aperture

$$R(F, w, Z, A, \gamma) = \int_{-wA/2}^{wA/2} f(x, Z) dx - 2 \int_0^{wA/2} f(x, Z) dx = 2 \frac{\exp(j\pi/4) \exp(-j2\pi FZ)}{\sqrt{2}}$$

$$\int_0^{wA/2} [Ei^*(T^+(x)) - Ei^*(T^-(x))] dx \quad (27)$$

where  $T = \frac{\pi F(x \pm A/2)^2}{Z|1 + \gamma|}$

so that

$$dx = \frac{1}{2} \sqrt{\frac{Z|1 + \gamma|}{\pi F}} \cdot \frac{1}{\sqrt{T \pm}}$$

$$/2) = U_{\pm} = \frac{\pi FA^2 (w \pm 1)^2}{4Z|1 + \gamma|} \quad (28)$$

Then

$$R(F, w, Z, A, \gamma) = 2 \frac{\exp(j\pi/4) \exp(-j2\pi FZ)}{\sqrt{2}} \cdot \frac{1}{2} \sqrt{\frac{Z|1 + \gamma|}{\pi F}} \left[ \int_0^{U_+} \frac{Ei^*(T)}{\sqrt{T}} dT - \int_0^{U_-} \frac{Ei^*(T)}{\sqrt{T}} dT \right] = \frac{\exp(j\pi/4) \exp(-j2\pi FZ)}{2\sqrt{2}}$$

$$\alpha [Ei^*(U_+) - Ei^*(U_-)] \quad (29)$$

where,

$$\alpha = \sqrt{\frac{Z|1 + \gamma|}{\pi FA^2}} \cdot \left( \frac{w + 1}{2} \right)^2$$

$$Ei^*(U_{\pm}) = \int_0^{U_{\pm}} \frac{Ei^*(T)}{\sqrt{T}} dT \quad (30)$$

Notice that each tap can have a sign as well as an amplitude, so this response should be multiplied by  $S_T S_R$ , where  $S_T$  and  $S_R = \pm 1$  are the signs

of the transmitting and receiving taps, respectively.

However,  $U_+ = U_+ - U_+ = U_+$

so that if  $Y = S_R W$  is the signed tap strength of the receiver,  $S_R [Ei^*(U_+) - Ei^*(U_-)] = Ei^*(V_+) - Ei^*(V_-)$

where

$$V_{\pm} = \left( \frac{Y_{\pm} + 1}{\alpha} \right)^2$$

Then the response, including tap signs, is

$$R(F, Y, S_T, Z, A, T) = S_T \frac{\exp(j\pi/4) \exp(-j2\pi FZ)}{2\sqrt{2}} \alpha [Ei^*(V_{nm+}) - Ei^*(V_{nm-})] \quad (31)$$

The total response is then the superposition of responses for each possible pair of transmitting and receiving taps. Indexing the transmitter by  $n$  and receiver by  $m$  (Fig. 5).

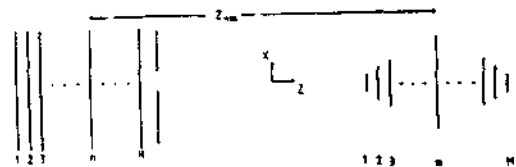


Fig. 5 - full filter model

$$T(F) = \sum_{n=1}^N \sum_{m=1}^M R(F, Y_m, S_n, Z_{nm}, A, \gamma)$$

$$= \frac{\exp(j\pi/4)}{2\sqrt{2}} \sum_{n=1}^N S_n \sum_{m=1}^M \alpha_{nm} [Ei^*(V_{nm+}) - Ei^*(V_{nm-})] \exp(-j2\pi FZ_{nm}) \quad (32)$$

where

$$V_{nm\pm} = \left( \frac{Y_{m\pm} + 1}{\alpha_{nm}} \right)^2, \quad \alpha_{nm} = \sqrt{\frac{Z_{nm}|1 + \gamma|}{\pi FA^2}}$$

If the apodized taps are not centered symmetrically in  $X$ , then the response formula would be



$$R(F, w, c, Z, A, \gamma) = \int_{c-WA/2}^{c+WA/2} f(x, Z) dx$$

$$= \int_0^{c+WA/2} f(x, Z) dx - \int_0^{c-WA/2} f(x, Z) dx$$

$$= \frac{\exp(j\pi/4) \exp(-j2\pi FZ)}{2\sqrt{2}} \alpha^{-1/2}$$

$$(E_{fi}^*(U_{++}) - E_{fi}^*(U_{+-})) - E_{fi}^*(U_{-+}) - E_{fi}^*(U_{--}) \quad (3)$$

where,

$$U_{\pm \pm} = \left( \frac{C + Y_{\pm}^{-1}}{\alpha} \right)^2$$

#### IV. COMPUTER SIMULATION

The previously defined mathematical model for diffraction is applied to an analysis of a Surface Acoustic Wave bandpass filter using 11 pairs of unapodized interdigital transducer and 239 apodized IDTs. The IDT configuration is shown in Fig.6. The filter will be assumed to have nominally equally spaced taps with spacing of  $\lambda/B$  and the center spacing of  $13 \lambda_0$ . The material used is  $128^\circ \text{LiNbO}_3$  and its anisotropy parameter  $\tau$  is  $-0.43$ . The diffracted response is simulated taking into account the spatial layout of the taps depicted in Fig.7, on VAX8550 in FORTRAN programming language.

The result is plotted and compared with that of "no diffraction" case. The diffraction simulation procedure is shown in the next Flow Chart.

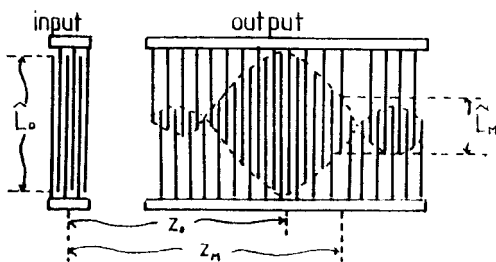


Fig. 6 IDT pattern for the bandpass filter

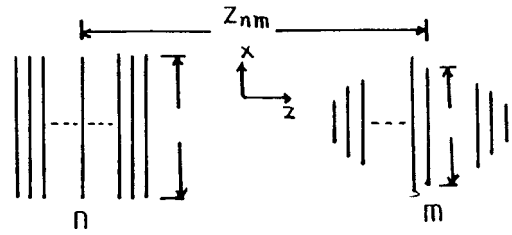


Fig. 7 layout of taps for diffraction calculation

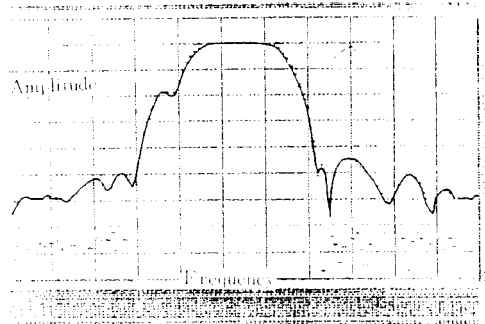


Fig. 8. The simulation result  
Solid line The response with diffraction  
dotted line The ideal response

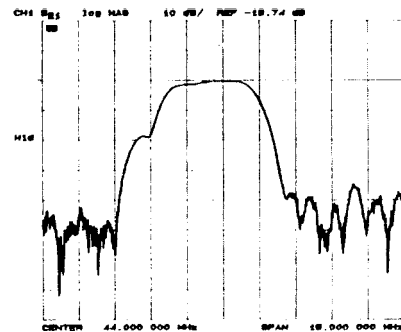
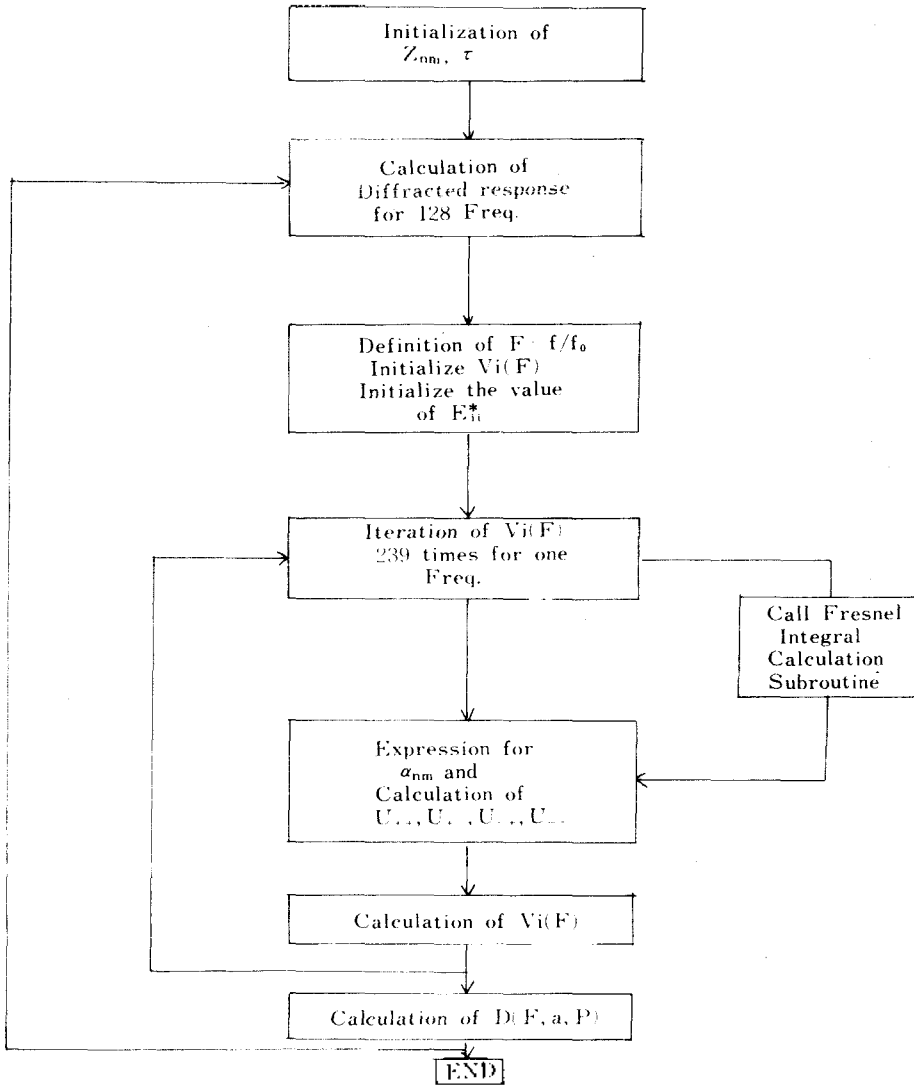


Fig. 9. The experimental result

#### V. RESULTS AND DISCUSSIONS

From the computer simulation result, it is shown that the passband region (41 MHz ~ 46 MHz) is less affected by the diffraction effects than the sidelobes, which is in complete agreement with the statement made earlier that regions where the finger overlap is small yield significantly more diffraction loss than that for the longer overlap. This is due to the fact that in an anisotropic propagation medium, the direc

DIFFRACTION SIMULATION PROCEDURE



tion of the phase and group velocity vectors does not always coincide with the propagation direction. Thus the acoustic beam tends to propagate off at an angle  $\phi$ , the power flow angle with respect to the centerline (propagation direction) between the two transducers.

In an ideal case where diffraction effects are not taken into consideration, the simulation result shows more than 70 dB drop in amplitude

in the sidelobe regions. However, the simulation with diffraction effects included reveals that there is only about 50 dB (or less) drop in amplitude. This is very significant in that 20 dB difference in amplitude will severely affect the filter performances. Furthermore, the higher frequency region is more affected than that of the lower frequency.

Mathematical model for the parabolic aniso-

trophy and the Fresnel approximation method has been derived and used to calculate the diffracted response of the Surface Acoustic Wave IF band-pass filter. The calculation of the diffracted response was simulated on VAX8550 in FORTRA and the result was plotted. On the same plot, "no-diffraction" response was also plotted so that a direct comparison could be made between the ideal case and the practical case. From this plot, one can easily see the effect of diffraction on the design of Acoustic Surface Wave filters. The severity of the diffraction effect in the stopband regions was observed and this is a major obstacle which must be overcome when designing Surface Acoustic Wave devices. Furthermore, the frequency response of the SAW IF bandpass filter for  $128^\circ$  Rotated  $\text{LiNbO}_3$  is given so that a direct comparison can be made with the simulation result. One can easily see that there is a remarkable similarity between the two plots with minor discrepancies. It can then be concluded that for the SAW IF bandpass filter for  $128^\circ$   $\text{LiNbO}_3$  with the center frequency of 44 MHz, the parabolic anisotropy and Fresnel approximation method gives a reasonably acceptable result for diffraction analysis. It should however be noted that the parabolic anisotropy and Fresnel approximation method does not provide us with an exact diffraction analysis because the slowness surface of  $128^\circ$   $\text{LiNbO}_3$  cannot always be approximated by a parabola. For more exact diffraction analysis, the angular spectrum of waves approach is required and the

detailed velocity profile must be known. In order to effectively carry out diffraction analysis, a faster diffraction computation algorithm is desired and this will in effect lead to a more appropriate diffraction compensation techniques.

## VII. REFERENCES

1. T.L. Szabo and A.J. Slobodnik, Jr., "The effect of Diffraction on the design of Acoustic Surface Wave Devices," IEEE Trans. Ultrasonics, Vol. SU-20, pp.240-251, July 1973.
2. M.G. Cohen, "Optical Study of Ultrasonic Diffraction and Focusing in Anisotropic Media," J.A.P., Vol. 38, pp.3821-3828, 1967.
3. J.M. Stone, Radiation and Optics, McGraw-Hill, New York, 1963.
4. M.S. Kharusi and G.W. Farnell, "Diffraction and Beam Steering for Surface-Wave Comb Structures on Anisotropic Substrates." IEEE Trans. on Sonics and Ultrasonics, Vol. SU-18, pp.35-42, 1971.
5. E.B. Savage, "Compensation for nonideal effects in surface acoustic wave interdigital filters," Ph.D. dissertation, University of California, Santa Barbara, June 1980.
6. M. Tan and C. Flory, "Fast computation of SAW diffraction by asymptotic techniques," IEEE Trans. Ultrason., Ferroelectrics, Frequency Contr., Vol. UFFC-2, pp.93-104, Jan., 1987.
7. W.A. Radasky and G.L. Matthaei, "Fast computation of diffraction in general anisotropic media by use of the geometrical theory of diffraction," IEEE Trans. Sonics Ultrason., Vol. SU-30, pp. 78-84, Mar., 1983.

▲ Yeong Jee Chung



- Born on Oct. 22nd, 1959 in Seoul
- Received B.S and M.S degree in Electrical Engineering from Yon Sei University in Feb, 1982 and Feb. 1984, respectively
- Currently enrolled in Ph.D program at Yon Sei University
- Have been working on SAW devices at Samsung Advanced Institute of Technology since July, 1987.

▲ Kyo Young Jin



- Born on Feb. 18th, 1962 in Seoul
- Received B.E. and M.E. degree in Electrical Engineering from Stevens Institute of Technology (NJ, U.S.A) in May, 1984 and May, 1986, respectively
- Have been working at Samsung Advanced Institute of Technology since July, 1977.